Relative stability and elastic properties of hcp, bcc, and fcc beryllium under pressure

G. V. Sin'ko* and N. A. Smirnov
Russian Federal Nuclear Center, Institute of Technical Physics, 456770, Snezhinsk, Russia
(Received 13 November 2004; revised manuscript received 17 February 2005; published 28 June 2005)

Ab initio electronic-structure calculations, based on the density-functional theory and the full-potential linear-muffin-tin-orbital method, were used to predict crystal-sructure phase stabilities and elastic constants of beryllium under compression. Specific energies, pressures, elastic constants, and Debye temperatures for three crystal structures, hcp, bcc, and fcc, were calculated over a wide volume range. In agreement with experiments and previous theoretical calculations, the hcp ground state is obtained at ambient conditions and the bcc ground state is found at high pressure and ambient temperature, with the predicted hcp→bcc phase transition at about 2.7 Mbar. A possible phase diagram of beryllium, including hcp, bcc, and fcc phases is constructed in the (P,T) plane.

DOI: 10.1103/PhysRevB.71.214108 PACS number(s): 62.20.Dc, 62.50.+p, 64.30.+t, 64.70.Kb

I. INTRODUCTION

The interest to beryllium (Be) arises from the fact that despite its simple atomic structure this material exhibits a number of unusual physical properties. Under ambient conditions, Be crystals have a hcp structure with the axial ratio $c/a=1.568$ that significantly differs from the ideal value equal to 1.633. High Debye temperature (1440 K) and very small Poisson's ratio (0.05) of hcp Be suggest that the behavior of valence electrons deviates substantially from that of near free electrons. At 1530 K Be transforms into the bcc structure which melts at 1560 K. The negative slope of the hcp→bcc phase boundary ($dT_{hcp\rightarrow bcc}/dP<0$) under compression points to the possibility of a hcp→bcc transition at high pressure and ambient temperature. Uncertainty in the value of Debye temperature for Be added another intrigue. In Ref. 1, a value of 897 K is recommended although it is much lower than 1440 K (Ref. 2) used earlier. According to recently published data,[3] Debye temperature at ambient conditions is equal to 1453 K. These differences are of great importance for the analysis of results obtained in *ab initio* calculations because the value of Debye temperature reflects the zero-point contribution to the total energy.

So it is no wonder that Be attracts attention of many scientists. The features of the electron distribution in Be were theoretically studied in Refs. 4 and 5. It was found that the electronic structure of Be was quite different from that of other divalent metals. The macroscopic properties of Be crystals at ambient pressure were studied using most known methods of electronic structure calculations.[6–15] The general inference is that results obtained with the *ab initio* methods reasonably agree with one another and with experiment but poorly agree with calculations based on the model potentials.

The number of theoretical papers devoted to the macroscopic properties of Be under pressure is much fewer, and most of them are devoted to the determination of the sequence of polymorphous transitions under pressure. Calculations[16–19] show that the structural transition in Be at $T=0$ K is possible in the pressure range of 1–2 Mbar. The cited works used LMTO-ASA,[16] *ab initio* pseudopotentials,[17] ASW,[18] and FPLMTO,[19] and the calculations were made in the local density approximation without gradient corrections. The authors of Refs. 16 and 18 predict that the hcp→bcc transition occurs, while those of Ref. 17 report that under pressure both the structures, bcc and fcc, are more favored than hcp. However, the accuracy of calculations[17] was not sufficient to determine the relative stability of these structures. In Ref. 19, the crystal structure stability among the hcp, bcc, and orthorhombic (distorted hcp) structures was studied as a function of compression. The bcc structure was found to be energetically stable at pressures above 1.8 Mbar.

A number of experiments were made to locate the hcp →bcc transition at ambient temperature. In spite of first optimistic results,[20–22] later experiments[23–26] failed to find this transition at pressures up to 1.71 Mbar.

And finally, in the recent paper[27] it is predicted that the shear modulus of all metals, including Be, vanishes at high pressure and absolute zero temperature and crystalline material becomes liquid.

In this paper we investigate the electronic structure and elastic properties of hcp, bcc, and fcc Be under pressure on the basis of one of the advanced methods of *ab initio* electronic structure calculations—FPLMTO.[28] Using the modified Debye model[29] to estimate the contribution of zero-point vibrations and thermal terms to Be thermodynamic functions, we determine the pressure of the hcp→bcc transition at ambient temperature and construct a possible phase diagram of Be in the (P,T) plane solely on the basis of *ab initio* calculations. We also calculate elastic constants for three Be structures as functions of relative volume, and check the hypothesis[27] that the shear modulus of Be crystals vanishes at high pressures.

II. DETAILS OF CALCULATIONS

We used the density-functional theory and the full-potential linear-muffin-tin-orbital method (FP-LMTO)[28] in the calculations reported here. The exchange-correlation functional in form offered in Ref. 30 with the gradient corrections[31] was used. This form of the exchange-correlation functional was chosen to describe the properties of Be crystals under ambient conditions as accurately as pos-

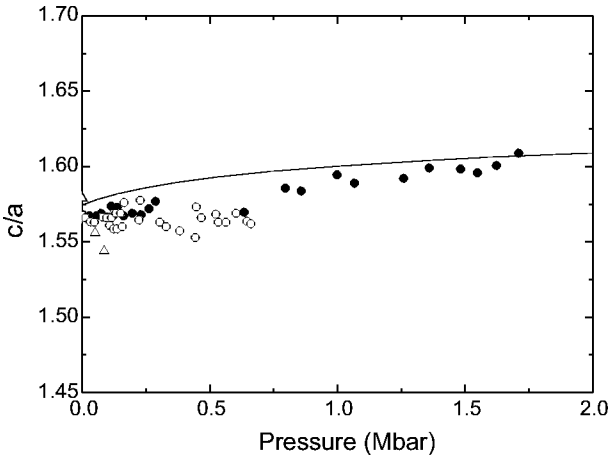

FIG. 1. The calculated axial ratio c/a as a function of pressure for hcp Be (solid line) compared with experimental data: triangle—Ref. 21, open circle—Ref. 25, filled circle—Ref. 26.

sible. All electrons were included into a fully hybridized energy panel. The basis set comprised augmented linear muffin-tin orbitals with s, p, and d momenta. We used eight centers of linearization for basis functions in the muffin-tin spheres and three tail energies in the interstitial region.[28] The values of these parameters for different specific volumes were chosen with a special automatic algorithm that allowed for a pressure dependence of the crystal energy spectrum. In the prism-shaped Brillouin zone a mesh for integration over k space with the linear tetrahedron method was constructed by dividing each edge into the same number of parts. The calculations were made with a $23\times23\times23$ mesh for all structures, both equilibrium and distorted. As a result of our effort aimed to choose the inner parameters of the FP-LMTO method,[28] we have succeeded to calculate the specific energy of the crystal accurately to 0.1 mRy/cell for all considered compressions. This means that changes in the inner parameters of the method, including the parameters that define the quality of the basis, can reduce the calculated unit cell energy by no more than 0.1 mRy. That value does not coincide with the absolute error in the total energy [relative to the exact local density approximation (LDA)/GGA result]. The energy convergence criterion that defines the number of iterations of the self consistent loop, was taken to be 10^{-3} mRy/cell. The pressure versus volume dependence at $T=0$ K was calculated by differentiation of an analytical expression which approximated the specific energy-volume dependence. To calculate pressure at a point of the V/V_0 mesh, we approximated specific energy over the interval containing four neighbor points, using the formula proposed in Ref. 32. Elastic constants for crystals under pressure were calculated with a method described in detail in Ref. 29.

III. RESULTS

The specific energy of each phase was calculated at 17 volume points between $V/V_0=1.1$ and $V/V_0=0.3$. Here $V_0=54.75$ $(\mathrm{a.u.})^3$/atom is the specific volume of Be at ambient pressure and room temperature, calculated from the experimental lattice parameters:[33] $a=2.2850$ Å, $c=3.5847$ Å. The equilibrium value of the axial ratio c/a for each specific volume of hcp Be was found from the condition of specific energy minimum as a function of c/a at constant volume. Figure 1 shows the obtained pressure dependence of the ratio c/a in comparison with experimental results. It is seen that the calculated and experimental data agree satisfactorily.

TABLE I. Experimental and calculated equilibrium volumes, V_0, ratio c/a, bulk modulus B_0, and pressure derivative of bulk modulus B_0' for hcp Be under ambient conditions.

	T=298 K experiment	T=0 K calculation without zero-point vibrations	T=298 K calculation with zero-point vibrations
V_0, $\frac{(\mathrm{a.u.})^3}{\mathrm{atom}}$	54.75,[a] 54.78[b]	53.46	54.44
c/a	1.569,[a] 1.568[b]	1.573	
B_0, Mbar	1.1,[c] 1.14,[d] 1.18,[e] 1.19[f]	1.22	1.14
B_0'	4.6,[c] 3.52,[e] 3.48[f]	3.306	4.34

[a]From Ref. 33, static.
[b]From Ref. 34, static.
[c]From Ref. 35, static.
[d]From Ref. 36, static.
[e]From Ref. 37, shock.
[f]From Ref. 38, shock.

To evaluate the accuracy of our calculations, we calculated some Be parameters under ambient conditions. They are given in Tables I and II with corresponding experimental results. The contribution of lattice thermal vibrations to the calculated quantities at $T=298$ K were defined using the Debye model.[29] As seen from Tables I and II, the calculated quantities are in good agreement with experiment.

As shown in Ref. 29, for elastic constants at $P\neq0$, it is natural to use the quantities $\tilde{C}_{ij}$, that are related to the elastic constants C_{ij}, traditionally defined as

$$C_{ij}=\frac{1}{V}\left.\frac{\partial^2 E(V,\{\eta_m\})}{\partial\eta_i\,\partial\eta_j}\right|_{\{\eta_m=0\}}, \tag{1}$$

via the following relations:

$$\tilde{C}_{ii}=C_{ii}-P,\quad i=1,2,\ldots,6;$$

TABLE II. Calculated elastic constants Be at $T=0$ K, $V=V_0$. The corresponding experimental results has obtained at ambient temperature (295 K) (see Ref. 3).

Elastic constants (Mbar)	Experiment	Calculation without zero-point vibrations
C_{11}	2.936	3.008
C_{33}	3.567	3.595
C_{44}	1.662	1.602
C_{12}	0.268	0.141
C_{13}	0.140	0.071

TABLE III. Second-order elastic constants for hcp Be at different relative volumes.

V/V_0	$\tilde{C}_{11}$ (Mbar)	$\tilde{C}_{33}$ (Mbar)	$\tilde{C}_{44}$ (Mbar)	$\tilde{C}_{12}$ (Mbar)	$\tilde{C}_{13}$ (Mbar)
1.1	2.320	2.805	1.370	-0.030	-0.046
1.0	3.008	3.595	1.602	0.141	0.071
0.8	5.044	6.162	2.269	1.065	0.496
0.6	9.451	11.69	3.419	3.331	1.779
0.5	13.74	17.56	4.375	6.174	3.140
0.4	21.25	27.63	5.739	11.96	6.178
0.3	36.86	48.86	7.807	24.78	14.00

$$\tilde{C}_{ij} = C_{ij}, \quad i = 1,2,3; \quad j = 4,5,6;$$

$$\tilde{C}_{12} = C_{12} + P, \quad \tilde{C}_{13} = C_{13} + P, \quad \tilde{C}_{23} = C_{23} + P;$$

$$\tilde{C}_{45} = C_{45}, \quad \tilde{C}_{46} = C_{46}, \quad \tilde{C}_{56} = C_{56}. \tag{2}$$

Here η_i are Lagrangian strains. If use $\tilde{C}_{ij}$ instead of C_{ij}, the usual Born conditions of mechanical stability remain valid for any pressure.[29] Tables III and IV contain $\tilde{C}_{ij}$ as functions of relative volume for hcp, bcc, and fcc Be at $T=0$ K.

It is of interest to note that according to our calculations, bcc Be becomes mechanically unstable somewhere on an interval $1.05 < V/V_0 < 1.10$. Accuracy of our calculations is not sufficient to confidently determine the value of V/V_0 at which the mechanical stability is lost but it is clear that this occurs at a density, which is a little lower than the ambient one. The elastic properties of bcc Be dramatically change near this boundary and, as a consequence, the contribution of nuclei thermal vibrations to the crystal thermodynamic functions changes. In our opinion this is the reason why the slope of the hcp→bcc phase boundary (dT/dP) of the Be crystal is so sharply negative at small compressions. This can be proved by the following estimation. The change in the temperature of the hcp→bcc transition, caused by the change in the Debye temperature of the bcc structure at constant pressure, can be written, accurately to linear terms, as

$$\Delta T_{hcp\to bcc} = -\frac{\left.\frac{\partial G_{bcc}}{\partial \Theta_D}\right|_{P,T} \Delta\Theta_D^{bcc}}{\left.\frac{\partial G_{hcp}}{\partial T}\right|_{P,\Theta_D} - \left.\frac{\partial G_{bcc}}{\partial T}\right|_{P,\Theta_D}}. \tag{3}$$

It is also possible to show that in Debye model

$$\left.\frac{\partial G}{\partial \Theta_D}\right|_{P,T} > 0. \tag{4}$$

Furthermore, our calculations show that near the hcp→bcc transition line

$$\left.\frac{\partial G_{hcp}}{\partial T}\right|_{P,\Theta_D} < \left.\frac{\partial G_{bcc}}{\partial T}\right|_{P,\Theta_D}. \tag{5}$$

So, one can expect that the sharp decrease of Debye temperature of the bcc structure near ambient pressure, caused by the loss of mechanical stability by this structure at small negative pressures, will result in a sharp increase of the hcp→bcc transition temperature, and just this is observed in experiment.

Using data contained in Tables III and IV and the method offered in Ref. 29, we calculated Debye temperature as a function of relative volume for the three Be structures. The results are presented in Table V.

We also calculated the 300 K isotherm for hcp Be. It is shown in Fig. 2 along with data from static and shock experiments.[21,25,26,37] As seen from Fig. 2, the calculated iso-

TABLE IV. Second-order elastic constants for bcc and fcc Be at different relative volumes.

V/V_0	$\tilde{C}_{11}^{bcc}$ (Mbar)	$\tilde{C}_{12}^{bcc}$ (Mbar)	$\tilde{C}_{44}^{bcc}$ (Mbar)	$\tilde{C}_{11}^{fcc}$ (Mbar)	$\tilde{C}_{12}^{fcc}$ (Mbar)	$\tilde{C}_{44}^{fcc}$ (Mbar)
1.10				1.620	0.333	0.659
1.05	1.131	0.785	1.412			
1.00	1.468	0.908	1.852	2.027	0.600	1.458
0.90	2.055	1.300	2.518	2.630	1.010	2.360
0.80	2.915	1.864	3.123	3.501	1.599	3.091
0.70	4.202	2.731	4.003	4.783	2.479	4.036
0.60	6.235	4.145	5.235	6.772	3.926	5.314
0.50	9.693	6.617	7.111	10.12	6.472	7.320
0.40	16.44	11.31	10.15	16.35	11.45	10.62
0.30	30.89	22.11	15.47	29.77	22.85	16.40

TABLE V. Debye temperatures for hcp, bcc, and fcc Be at different relative volumes.

V/V_0	Θ_D^{hcp}(K)	Θ_D^{bcc}(K)	Θ_D^{fcc}(K)
1.10	1351.1		980.58
1.05		879.73	
1.00	1465.9	1044.6	1228.5
0.90		1197.8	1409.9
0.80	1711.8	1354.8	1547.9
0.70		1541.7	1707.3
0.60	2058.5	1763.4	1891.5
0.50	2279.1	2044.6	2130.5
0.40	2520.6	2454.7	2446.2
0.30	2828.1	2989.0	2862.9

therm is in good agreement with data from Refs. 21 and 25. It satisfactorily agrees with the experimental data[26] up to 0.7 Mbar, however, progressively disagrees for higher pressures. The agreement between theoretical and experimental results may be better if take into account the corrections to the ruby pressure scale, proposed in Ref. 39. As shown in Ref. 39, the correction increases experimental pressures in samples, especially those above 1 Mbar. The paper[39] provides aluminum compression data obtained with and without the proposed corrections to the ruby scale. Figure 3 shows these data and results of our calculations on the pressure-volume dependence for fcc Al.[29] It is seen that the experimental results obtained with the corrected ruby scale are in excellent agreement with our calculations. It seems reasonable to expect that the agreement between calculated and experimental results for Be will also be better if use the corrected ruby scale. As for the isotherm obtained from the experimental shock compression data,[37] it is seen to noticeably deviate from both static data[25,26] and our results at pressures above 0.5 Mbar. As noticed in Ref. 25, this may be a result of inaccuracy in the Gruneisen parameter used in experimental data processing.

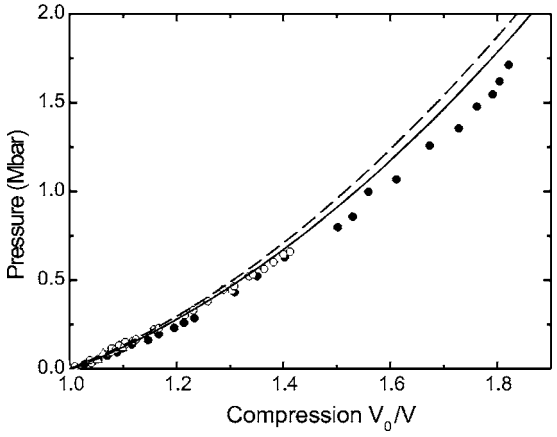

FIG. 2. The calculated 300 K isotherm for hcp Be (solid line) compared with experimental data: triangle—Ref. 21, open circle—Ref. 25, filled circle—Ref. 26; the dashed line is the room temperature isotherm derived from experimental shock-wave measurements (see Ref. 37).

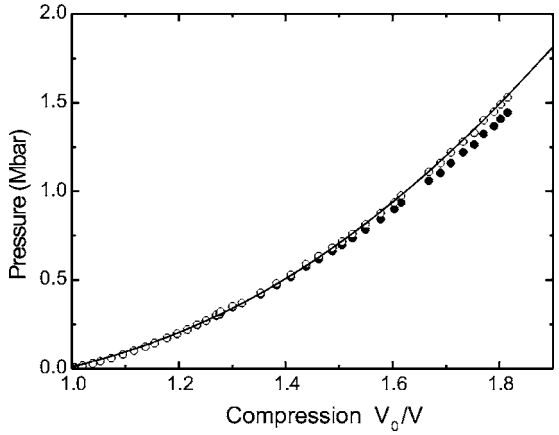

FIG. 3. Calculated (see Ref. 29) pressure-volume relation for fcc Al (solid line) compared with experimental data (see Ref. 39): open circle—modified ruby pressure scale, filled circle—old ruby pressure scale (see Ref. 40).

Using the elastic constants obtained, we calculated shear moduli G for the three structures of Be polycrystal with the formula

$$G = \tfrac{1}{2}(G_V + G_R). \tag{6}$$

Here G_V and G_R are polycrystal shear moduli obtained by averaging the single-crystal elastic constants $\tilde{C}_{ij}$ as proposed by Voigt[41] and Reuss,[42] respectively. G_V is the upper bound for the polycrystal shear modulus and G_R is the lower one. Formulas for G_V and G_R under pressure can be found in Ref. 43.

Figures 4, 5, and 6 show the polycrystal shear modulus G and single-crystal shear moduli $\mu=(\tilde{C}_{11}-\tilde{C}_{12})/2$ and $\mu'=\tilde{C}_{44}$ for the three Be structures as functions of pressure at $T=0$ K. It is seen that none of the moduli becomes zero to at least 10 Mbar.

The author of Ref. 27 discusses possible melting of crystals under isothermal compression as a result of shear modulus vanishing. According to the estimation Ref. 27, the shear modulus of Be vanishes at pressures above 1.1 Mbar. Since

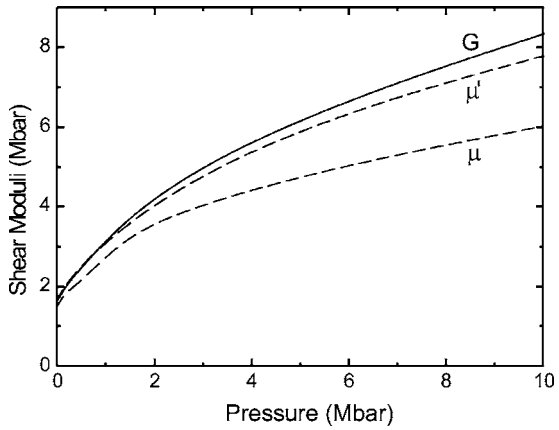

FIG. 4. Shear modulus of polycrystals and single-crystals of hcp Be as functions of pressure.

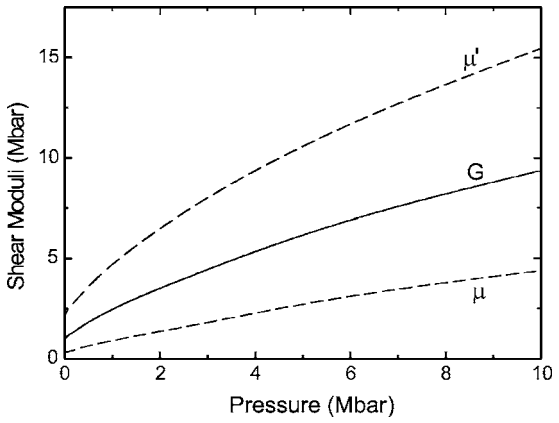

FIG. 5. Shear modulus of polycrystals and single crystals of bcc Be as functions of pressure.

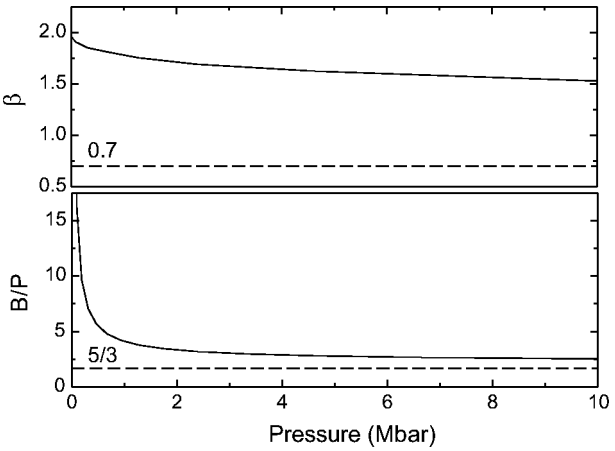

FIG. 7. Pressure dependence of β and B/P for bcc Be.

this result disagrees with what we obtained, consider this estimation in more detail. In that paper the shear modulus G_V is calculated as

$$G_V = \tfrac{3}{5}(\beta B - 2P), \tag{7}$$

were B is bulk modulus, P is pressure. The author of Ref. 27 assumes that the value of $\beta = 1 - (\tilde{C}_{12} - \tilde{C}_{44} - 2P)/B$ is constant and close to its magnitude for cubic metals under ambient conditions: $\beta = 0.7$. Then, following from the fact that at high pressures $B/P \to 5/3$, he makes the conclusion that G_V turns negative at high pressures. Using for B and P the expressions that approximate the results of calculation of thermodynamic functions by the Thomas-Fermi model with corrections, the author[27] finds that for Be, $G_V < 0$ at $P > 1.1$ Mbar. At the same time he notes that the result is very sensitive to the value of the parameter beta and should be considered qualitative.

Figure 7 shows the pressure dependence of β and B/P we calculated for bcc Be. It is seen from Fig. 7 that the ratio B/P does approach 5/3 in the high compression limit, as it must be. However, for bcc Be, the value of β is not close to 0.7 either at low or high pressures and therefore, G_V remains positive. For many cubic metals under ambient conditions, β differs from 0.7 too. So, for example, for Ca, $\beta \approx 1.22$ and for Tl, $\beta \approx 0.32$. Thus, the qualitative conclusion[27] on the behavior of the shear modulus of metals under pressure cannot be admitted to agree with results of *ab initio* calculations. Taken alone, the vanishing of the shear modulus of a crystalline structure at $T = 0$ K only means that the structure loses its mechanical stability. For the structure to transform into liquid, the Gibbs potential of the liquid phase must be lower than that of any other crystalline structure. The possibility of the solid-liquid transition cannot be *a priori* ruled out but it is unlikely to be general for practicable pressures.

Using the modified Debye model,[29] we calculated Gibbs potentials for hcp, bcc, and fcc Be as functions of pressure at $T \geqslant 0$. They were used to predict the pressure of the possible hcp $\to$ bcc transition at room temperature and obtain the possible phase diagram for Be in the (P,T) plane. Figure 8 shows the pressure dependence of Gibbs potentials for the considered structures of Be relative to the Gibbs potential of the hcp structure at 300 K. It is seen that the hcp structure is most favored under ambient conditions and remains so up to a pressure of 2.7 Mbar where the hcp $\to$ bcc transition occurs. Then, at least up to 10 Mbar, the bcc structure remains

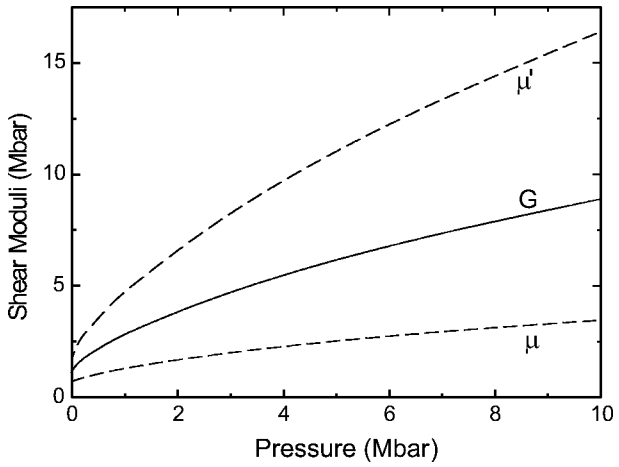

FIG. 6. Shear modulus of polycrystals and single crystals of fcc Be as functions of pressure.

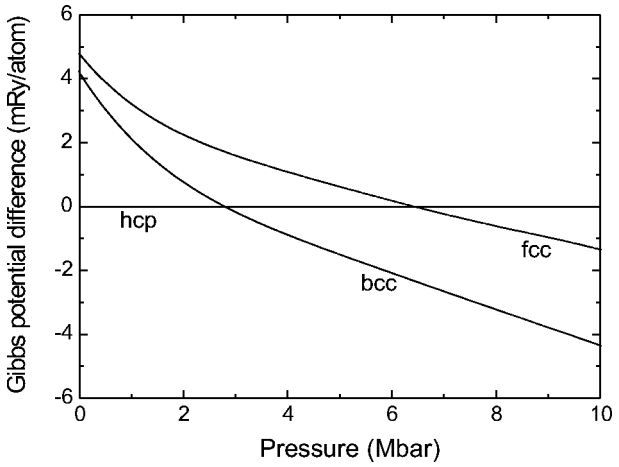

FIG. 8. Gibbs potential differences of bcc and fcc Be with respect to hcp Be at $T = 300$ K as functions of pressure.

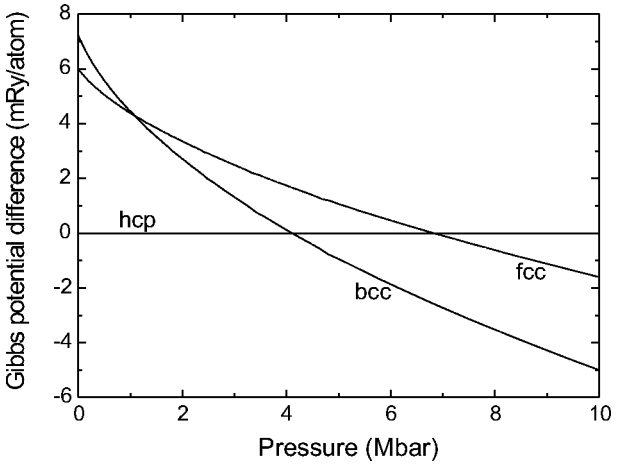

FIG. 9. Gibbs potential differences of bcc and fcc Be with respect to hcp Be at $T=0$ K as functions of pressure without zero-point contribution to the Gibbs potential.

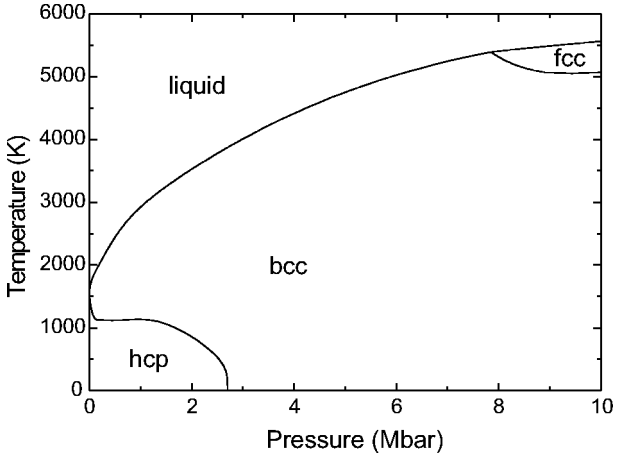

FIG. 10. A possible phase diagram of Be, including hcp, bcc, and fcc phases. The melting curve was calculated from the Lindeman criterion (8).

most favored. Our estimate of the hcp→bcc transition pressure equal to 2.7 Mbar does not contradict the experimental data[25,26] but is higher than the values calculated in Refs. 16–19.

It is interesting to see how functions in Fig. 8 will change if neglect the contribution from the thermal motion of nuclei and zero-point vibrations. In this case our results can be directly compared with results presented in Refs. 16–19. For this end we present Fig. 9 which shows our calculations on the Gibbs potential differences of bcc and fcc structures with respect to the Gibbs potential of the hcp structure in the case where $T=0$ K and the contribution of zero-point vibrations is not taken into account. It is seen that in this case at $P=0$, the hcp structure is again most stable. But now it remains most stable to a pressure of 4.1 Mbar and then turns into the bcc structure which remains stable to at least 10 Mbar. The pressure of the hcp→bcc transition we determined differs from ~ 2, ~ 5, ~ 3, ~ 1.8 Mbar obtained in Refs. 16–19, respectively. This is apparently a result of our using gradient corrections to the LDA exchange-correlation energy functional. It should be noted that with no account for the contribution from the motion of nuclei, the fcc structure at low pressures was found to be more stable than the bcc structure both in our calculations and in those presented in Refs. 16–19. Accounting for the contribution from the motion of nuclei, which differs for bcc and fcc structures if the method[29] is used, allows obtaining, at relatively low pressures and increasing temperature, a sequence of structural transformations that agrees with experiment.

Figure 10 shows the possible phase diagram for Be in the (P,T) plane. It includes the hcp, bcc, and fcc structures. The melting curve was calculated with Lindemann criterion

$$T_m = \text{const} \times V^{2/3}\Theta_D^2(V). \tag{8}$$

The constant in this equation was chosen using the experimental value of the melting temperature at ambient pressure. To reproduce the experimental phase boundary of hcp and bcc structures at pressures below 0.06 Mbar and high temperatures, we had to slightly correct the curve approximating the calculated pressure dependence of Debye temperature near $P=0$ for these structures. The corrections are within the calculation error, and they are no greater than 5% of the initial values. It should be emphasized that the qualitative result, the dramatic change of $dT_{hcp\to bcc}/dP$ near normal density, was obtained without any correction to the calculated data. A minor correction was only needed to match the calculated and experimental curves $T_{hcp\to bcc}(P)$.

IV. CONCLUSION

The specific energy, elastic constants, shear moduli, and relative stability of hcp, bcc, and fcc Be at pressures up to 10 Mbar were determined using *ab initio* electronic-structure FP-LMTO calculations. Our results showed that at $T=0$ K none of the structures became mechanically unstable, at least up to 10 Mbar. The obtained elastic constants were used to include the contribution of nuclei thermal oscillations to the equation of state of Be. The calculated Be crystal characteristics at ambient conditions and the 300 K isotherm agree well with the experimental data available. Our calculations suggest that at room temperature the structural hcp→bcc transition in Be occurs at a pressure of about 2.7 Mbar. The calculated data were used to construct the possible phase diagram for Be, including hcp, bcc, and fcc phases in the (P,T) plane.

ACKNOWLEDGMENT

This work was supported by the Russian Foundation for Basic Research (Grant No. 04-02-17292).

*Electronic address: gevas@uniterra.ru

[1] N. Gopi Krishna and D. B. Sirdeshmukh, Acta Crystallogr., Sect. A: Found. Crystallogr. **54**, 513 (1998).
[2] *American Institute of Physics Handbook*, 3rd ed. (McGraw-Hill, New York, 1972), Tables 4e-10 and 7b-1.
[3] A. Migliori, H. Ledbetter, D. J. Thoma, and T. W. Darling, J. Appl. Phys. **95**, 2436 (2004).
[4] U. Haussermann and S. I. Simak, Phys. Rev. B **64**, 245114 (2004).
[5] G. K. H. Madsen, P. Blaha, and K. Schwarz, J. Chem. Phys. **117**, 8030 (2002).
[6] J. F. Janak, V. L. Moruzzi, and A. R. Williams, Phys. Rev. B **12**, 1257 (1975).
[7] S. Chatterjee and P. Sinha, J. Phys. F: Met. Phys. **5**, 2089 (1975).
[8] F. Perrot, Phys. Rev. B **21**, 3167 (1980).
[9] R. Dovesi, C. Pisani, F. Ricca, and C. Roetti, Phys. Rev. B **25**, 3731 (1982).
[10] M. Y. Chou, P. K. Lam, and M. L. Cohen, Phys. Rev. B **28**, 4179 (1983).
[11] J. Redinger, K. Schwarz, N. K. Hansen, G. E. W. Bauer, and J. R. Schneider, Hahn-Meltner Institute, Berlin, Report HMI B412, 1984, pp. 79–99.
[12] U. von Barth and A. C. Pedroza, Phys. Scr. **32**, 353 (1985).
[13] P. Blaha and K. Schwarz, J. Phys. F: Met. Phys. **17**, 899 (1987).
[14] J. C. Boettger, J. Quantum Chem. symp. **29**, 197 (1995).
[15] N. A. W. Holzwarth and Y. Zeng, Phys. Rev. B **51**, 13653 (1995).
[16] A. K. McMahan, in *Shock Waves in Condensed Matter-1981*, AIP Conf. Proc. No. 78, edited by W. J. Nellis, L. Seaman, and R. A. Graham (AIP, New York, 1982), p. 340.
[17] P. K. Lam, M. Y. Chou, and M. L. Cohen, J. Phys. C **17**, 2065 (1984).
[18] J. Meyer-ter-Vehn and W. Zittel, Phys. Rev. B **37**, 8674 (1988).
[19] B. Palanivel, R. S. Rao, B. K. Godwal, and S. K. Sikka, J. Phys.: Condens. Matter **12**, 8831 (2000).
[20] A. R. Marder, Science **142**, 664 (1963).
[21] L. C. Ming and M. H. Manghnani, J. Phys. F: Met. Phys. **14**, L1 (1984).
[22] V. Vijayakumar, B. K. Godwal, Y. K. Vohra, S. K. Sikka, and R. Chidambaram, J. Phys. F: Met. Phys. **14**, L65 (1984).
[23] L. C. Chhabildas, J. L. Wise, and J. R. Asay, in *Shock Waves in Condensed Matter-1981*, AIP Conf. Proc. No. 78, edited by W. J. Nellis, L. Seaman, and R. A. Graham (AIP, New York, 1982), p. 422.
[24] R. L. Reichlin, Rev. Sci. Instrum. **54**, 1674 (1983).
[25] N. Velisavljevic, G. N. Chestnut, Y. K. Vohra, S. T. Weir, V. Malba, and J. Akella, Phys. Rev. B **65**, 172107 (2002).
[26] K. Nakano, Y. Akahama, and H. Kawamura, J. Phys.: Condens. Matter **14**, 10569 (2002).
[27] V. V. Kechin, J. Phys.: Condens. Matter **16**, L125 (2004).
[28] S. Yu. Savrasov and D. Yu. Savrasov, Phys. Rev. B **46**, 12181 (1992).
[29] G. V. Sin'ko and N. A. Smirnov, J. Phys.: Condens. Matter **14**, 6989 (2002).
[30] L. Hedin and B. I. Lundqvist, J. Phys. C **4**, 2064 (1971).
[31] J. P. Perdew, J. A. Chevary, S. H. Vosko, K. A. Jackson, M. R. Pederson, D. J. Singh, and C. Fiolhais, Phys. Rev. B **46**, 6671 (1992).
[32] G. Parsafar and E. A. Mason, Phys. Rev. B **49**, 3049 (1994).
[33] V. M. Amonenko, V. Ye. Ivanov, G. F. Tikhinskij, and V. A. Finkel, Phys. Met. Metallogr. **14**, 47 (1962).
[34] K. J. H. Mackay and N. A. Hill, J. Nucl. Mater. **8**, 263 (1963).
[35] D. J. Silversmith and B. L. Averbach, Phys. Rev. B **1**, 567 (1970).
[36] J. F. Smith and C. L. Arbogast, J. Appl. Phys. **31**, 99 (1960).
[37] J. L. Wise, L. C. Chhabildas, and J. R. Asay, in *Shock Waves in Condensed Matter-1981*, AIP Conf. Proc. No. 78, edited by W. J. Nellis, L. Seaman, and R. A. Graham (AIP, New York, 1982), p. 417.
[38] T. Neal, in *High Pressure Science and Technology*, edited by K. D. Timmerhaus and M. S. Barber (Plenum, New York, 1974), pp. 1 and 80.
[39] A. Dewaele, P. Loubeyre, and M. Mezouar, Phys. Rev. B **70**, 094112 (2004).
[40] H.-K Mao, J. Xu, and P. Bell, J. Geophys. Res. **91**, 4673 (1986).
[41] W. Voigt, *Lehrbuch der Krystall Physik* (Teubner, Leipzig, 1928), p. 962.
[42] A. Reuss, Z. Angew. Math. Mech. **9**, 49 (1929).
[43] D. L. Preston and D. C. Wallace, Solid State Commun. **81**, 277 (1992).